DFT calculations of Anatase TiO_2 (1 0 1) Surface Doped with Ruthenium for Application in Dye Sensitised Solar Cell

Nemudzivhadi[1] H., Maluta[1, 2] N.E., Maphanga[3] R.R., Sankaran[1]V.

[1]University of Venda, Department of physics, P/Bag X 5050, Thohoyandou, 0950

[2]National Institute for Theoretical Physics (NITheP), Gauteng, South Africa

[3]Material Modelling Centre, University of Limpopo P/Bag X 1106, Sovenga, 0727.

Email: hulisaninemudzivhadi@gmail.com

Abstract. Titanium dioxide (TiO_2) is considered to be an ideal semiconductor for photocatalysis because of its high stability, low cost and safety towards both humans and the environment. Doping TiO_2 with different elements has attracted much attention as the most important way of enhancing the energy band gap and the adsorption on different wavelength region, in order to improve the efficiency of the dye sensitized solar cells (DSSCs). In this study, first principle density function theory was used to investigate the reaction mechanisms between anatase TiO_2 (1 0 1) surface doped with ruthenium (Ru) atom as a dopant. Ru-doped anatase TiO_2 (1 0 1) surface was geometrically optimized using the generalized gradient approximation implemented within the CASTEP CODE. The calculated density of states and band structures for Ru-doped systems shows that the synergistic effects of Ru impurities at lattice titanium sites lead to a sharp band gap narrowed to 0.345 eV.

1. Introduction

The Energy is the basic resource of today's world. Along with the increase of the population, the demand of the amount of energy resource gets higher rapidly [1]. The solution to the growing demand and environmentally sustainable energy resources in the world might lie in the ability to capture and utilize renewable solar energy. To capture and utilize solar energy for a sustainable development on a large scale, development of cheaper technologies will be an added advantage [2]. In photovoltaic technologies, the DSSCs is a promising approach for direct conversion of sunlight into electrical energy at low cost and high-energy conversion efficiency [2]. The dye molecules as a sensitizer absorbs solar radiation and transfers the photo-excited electron to the wide band gap of TiO_2 semiconductor [3, 4]. The molecule dye is normally adsorbed on the surface of various TiO_2 polymorphs, which is usually on a nanometer size particle [3, 4]. Kamat reported that the inertness to chemical environment and long-term photostability has made TiO_2 an important material in many practical applications and in commercial products ranging from drugs to foods, cosmetics to catalysts, paints to pharmaceuticals and sunscreens to solar cells in which TiO_2 is used as a desiccant, brightener, or reactive mediator [5]. TiO_2 has an added advantage to be widely applied in the DSSCs because of its wide band gap [6]. But for the applications in paint material, the narrowing of the TiO_2 band gap is not desired. The problem encountered with the wide band gap of TiO_2 is that it crucially limits the practical application involving the photons absorption and electrons transport in DSSCs [7, 8]. To enhance the efficiency of DSSCs, it is essential to reduce band gap for TiO_2 material, such that the absorption properties will match well with visible solar spectrum [7- 10].

TiO_2 has three commonly known different structural types, which are rutile, anatase and brookite as shown in figure 1 [11]. All of these crystalline forms of TiO_2 occur in nature as mineral, but only rutile and anatase have been synthesized in pure form at low temperature [11]. Therefore, anatase and rutile phases, which are tetragonal crystal system, are widely studied, for their syntheses, characterizations and photocatalytic properties [9, 11]. So far, anatase phase is known to exhibit higher photocatalytic efficiency compared to rutile phase [12, 13]. Anatase is one of the most popular and promising materials in photocatalytic applications due to the strong oxidizing power of its holes, high photo stability and redox selectivity, with its band gap of (3.2 eV) [6, 11, 12, 13].

The light absorption is limited in the ultraviolet (UV) region because of the wide band gap, but Tian et al. reported that doping is a good approach to get a visible light driven photocatalyst [14]. The surfaces of TiO_2 play an important role in many technical applications, since Fujishima and Honda showed that photocatalytic water splitting is possible [15]. Recently Navrotsky showed that the anatase surfaces play an important role for the phase stability of TiO_2-nanoparticles [16]. Esch et al. studied the surfaces structures and thermodynamics of low-index of rutile, anatase and brookite, using density function theory (DFT) method [17]. The study investigated low-index surfaces of rutile, anatase and brookite by determining surfaces stability. It was reported that atomic relaxations of rutile (1 1 0), (1 0 0), anatase (1 0 1), (1 0 0) and brookite (2 1 0) surfaces, are the most common and most stable surfaces. Chen et al. investigated anatase TiO_2 (1 0 1) surface doped with O vacancies and nitrogen (N) atoms using DFT. The findings revealed that the mixing of O vacancies and N dopants induced state with original Ti 3d and O 2p valence band attributes to the band gap narrowing [18]. Using DFT method. Chen et al. reported that doping anatase (1 0 1) surface with sulfur lead to band gap narrowing as compared un-doped anatase TiO_2 systems [19]. Labt et al. and Mino et al. both they reported that anatase TiO_2 (1 0 1) surface is the only surface that can be modelled with even-n-layer slabs and the most stable surface of anatase [20, 21].

In this study, adsorption mechanisms for anatase TiO_2 (1 0 1) surface doped with Ru was investigated using DFT to calculate electronic properties and analyses.

2. Structures

Anatase TiO_2 has a tetragonal structure with (-space group: I 41 141/AMD. i.e., local symmetry: D19 4h/. The system is composed of four Ti atoms and eight O atoms in the primitive cell and its lattice parameters are a = b = 3.776 Å and c = 9.486Å) [11].

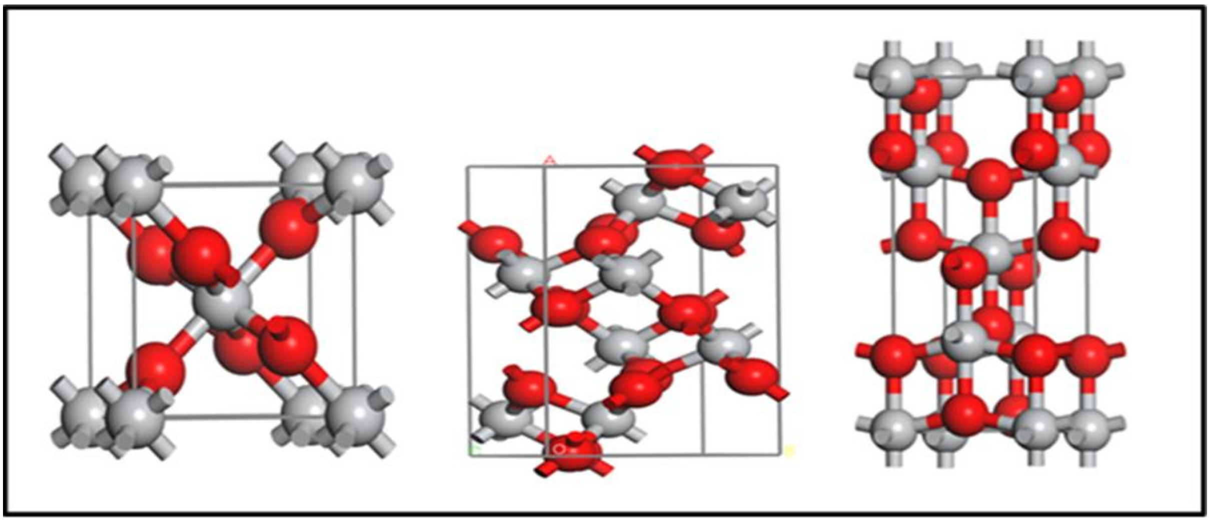

Figure 1. The primitive cells of rutile, brookite and anatase (from left to right), where the red balls and grey balls represent oxygen (O) and titanium (Ti) respectively.

3. Methodology and computational details

The first-principles calculations were performed using the Cambridge Serial Total Energy Package (CASTEP) code in materials studio developed by Accelrys Software Inc [22]. The energy plane-wave pseudopotential total calculation method based on DFT was used to carry out all the calculations. For structural optimization, the generalized-gradient approximation (GGA) with the Perdew-Burke Ernzerhof (PBE) exchange-correlation functional was employrd for all the calculations to obtain the electronic structures and accurate formations energies [22]. In these calculations, the energy cut-off for the plane-wave basis was set to be 600 eV and the Brillouin zone for the surface model was represented by a Monkhorst-Pack (MP) scheme for the generation of k-points of (4 x 6 x 1).

The convergence threshold for self-consistent tolerance was set to $2.0e^{-6}$ eV/atom and geometric relaxation was obtained with the Broyden-Fletcher-Goldfarb-Shanno (BFGS) algorithm until the atomic relaxations were below 0.05 eV/Å. The above mentioned parameters were suitable for getting well-converged total energy and geometry optimization results. In the geometry optimization, the convergence criteria for structural optimization were set to be medium quality with the energy change, maximum stress and maximum displacement of $2.0e^{-5}$ eV/atom, 0.1 GPqa and 0.002 Å, respectively. We cleaved surface with the fractional and angstrom thickness of 1.0 Å and 3.508 Å respectively and employ a slab unit cell with the same reconstruction on the top and bottom of the unit cell surface. In order to reduce the systematic error in comparing energies of different distances, we use the same computational setup as much as possible in all calculations. The vacuum orientation was c, thicknesses of the vacuum layers were 10.00 Å and crystal thickness was 13.3609 Å.

The doping effects were modelled by varying the distances between the ruthenium atom and atom on the anatase TiO_2 (1 0 1) surface. The Ru position was varied at an interval from 0.5 Å to 2.5 Å.

4. Results and discussion

Ru-doped anatase TiO_2 (1 0 1) surface were geometrically optimized until all the parameters were below the suitable tolerance for converged systems. The total energies as a function of Ru displacement are presented. Tables 1 present the initial (before geometry optimization) and final (after geometry optimization) atomic distance between the anatase TiO_2 (1 0 1) surface and the adsorbed Ru atom together with total energies. It is noted that Ru-doped atom is displaced away from the surface after optimizing with average bond distance between Ti and Ru atoms being 3.151 Å. The system that gave the most stable energy was then considered for further calculation on electronic properties. Thus, the optimized system whereby Ru atom was placed as 1.000 Å from the surface is considered and its surface structure is shown in Figure 2.

Total 1. Energies of the anatase TiO_2 (1 0 1) surface after optimization with Ru atom placed at various positions.

Initial distance (Å)	Final distance (Å)	Total energies (eV)
0.500	2.712	-7571.643
1.000	3.623	-7573.722
1.500	3.263	-7573.169
2.000	3.098	-7572.414
2.500	3.059	-7572.410

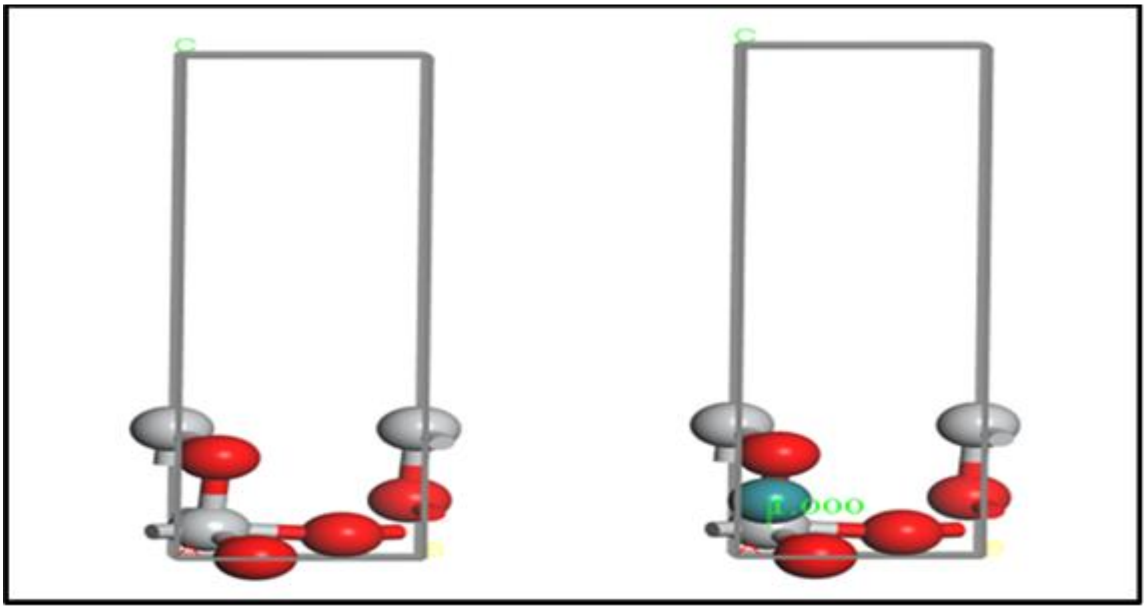

Figure 2. Cleaved structures of undoped and Ru-doped anatase TiO_2 (1 0 1) surface, where Ru adsorbed at a distance of 1.000 Å away from one Ti on the surface (from left to right).

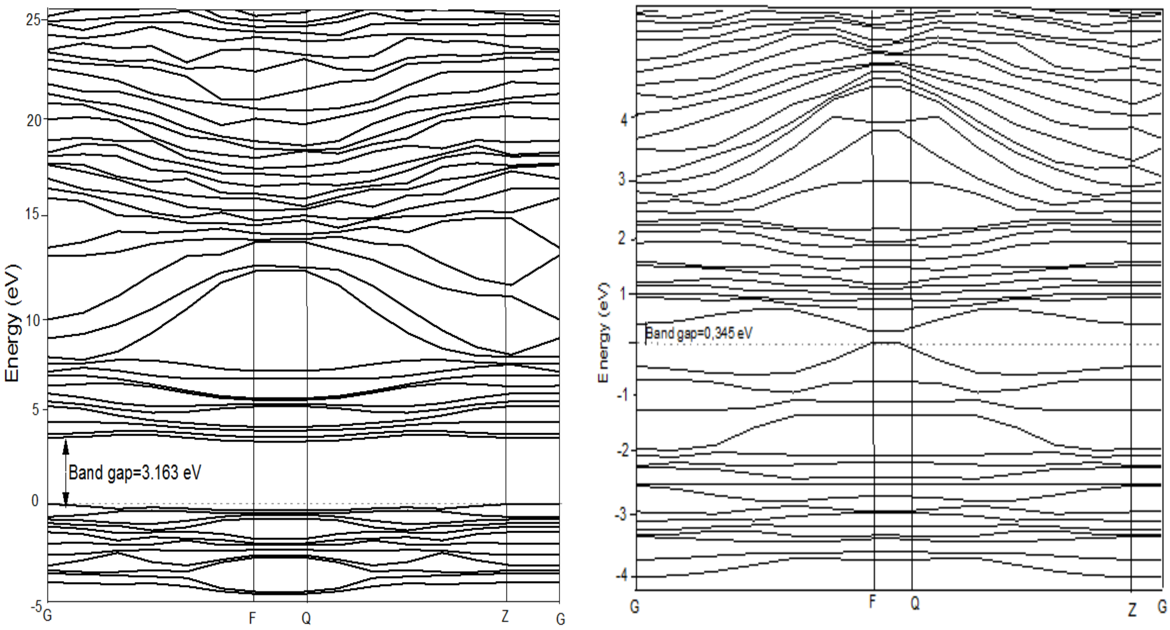

Figure 3. The band gaps of undoped and Ru-doped anatase TiO_2 (1 0 1) surface (from left to right).

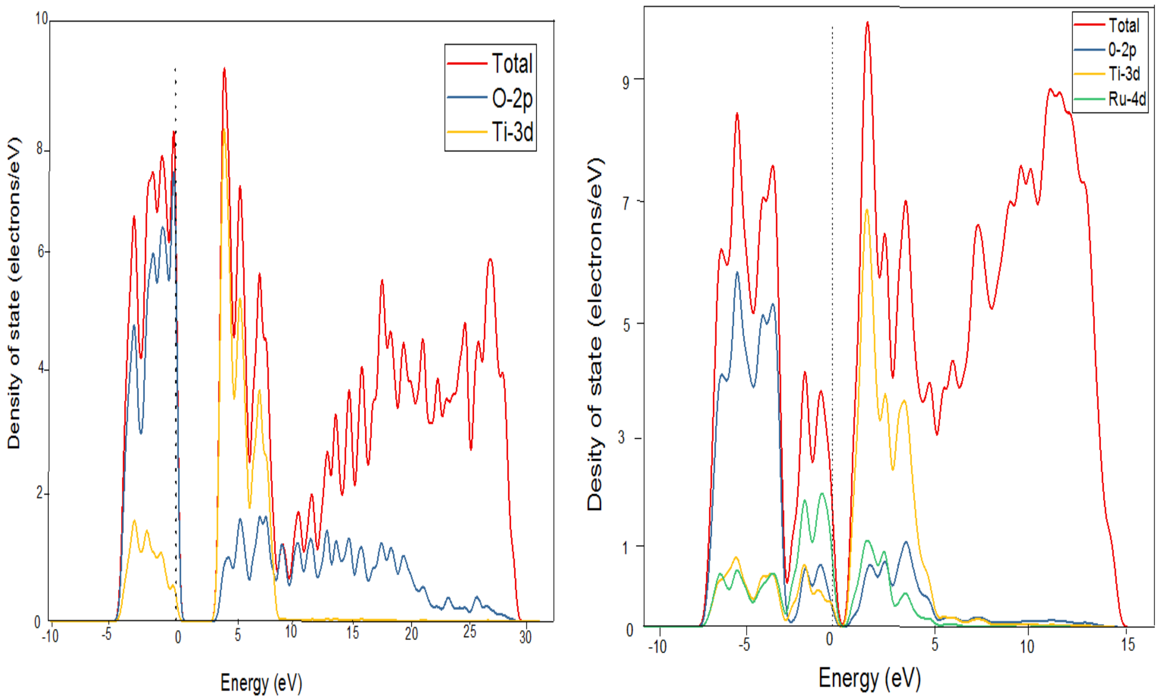

Figure 4. The partial and total density of state of undoped and Ru-doped anatase TiO_2 (1 0 1) surface (from left to right). Fermi level is at 0 eV.

To study the influence of doping on the electronic structures of TiO_2 (1 0 1) surface, the energy band structures of Ru-doped and undoping were calculated and shown in Figure 3. For undoped anatase (1 0 1) surface, the band gap was found to be 3.163 eV which is in agreement with results reported by [23], but with both lower than the experimental result of 3.230 eV [6, 11]. This difference of the calculated band gap from the experimental value can be due to the selection of exchange-correlation energy in DFT. For undoped system, the valance band (VB) near the Fermi level is mainly dominated by O 2p states and the conduction band (CB) is contributed by Ti 3d states, exhibiting that anatase TiO_2 has an indirect band gap. Moreover, Ru-doped systems show a pronounced narrowing of band gap to 0.345 eV as compared to band gap 3.163 eV of undoped (1 0 1) surface of anatase. Furthermore, the study suggests that the rate of the electron transferring from the VB to the CB is enhanced, due to the reduction in band gap doped system as compared to undoped system. The total density of states (TDOS) and partial density of states (PDOS) graph of undoped and Ru-doped TiO_2 is plotted in Figure 4. The valence band is dominantly composed of O 2p states and Ru 4d states while the conduction band is dominantly composed of Ti-3d. After doping the Fermi level is shifts near to the valence band, this shifts of the valence band indicate that Ru-doped anatase TiO_2 (1 0 1) surface is p-type semiconductor.

5. Conclusion

The energy plane-wave pseudopotential method implemented in DFT has been employed successfully to investigate the electronic properties of TiO_2 anatase (1 0 1) surface doped with Ru. When Ru atom is placed at various distance relative to Ti atom it prefer to move away from the surface suggesting a weaker bond between Ru and Ti. The calculations showed that doping TiO_2 with Ru-doping reduces the energy band gap. Thus calculated total and partial density of states for Ru-doped anatase TiO_2 (1 0 1) surface show a sharp decrease in the energy band gap from 3.163 eV to 0.345 eV, this is due to the synergistic effect of Ru.

6. Future work

Calculating optical properties (i.e. reflectivity, absorption, refractive index, dielectric function, conductivity and loss function) of undoped and Ru-doped anatase (1 0 1) surface. Investigating anatase TiO_2 low index surfaces [i.e. (1 0 0), (1 1 0), (1 1 1) and (1 0 1)] doped with other elements, such as alkaline-earth metallic (AEM) using substitution and adsorption methods and compare their electronic and optical properties results.

Acknowledgements

The financially supporter, from National Research Foundation (NRF). The University of Venda and University of Limpopo for the support to carry out this research. Centre for High performance Computing (CHPC) for using their facilities.

References

[1] Torres-Martínez J, Turner C, Uchiyama Y, Vuori S.J.V, Wamukonya N and Zhang X, (2007): In Climate Change, 4, 252-322.

[2] O'Regan B and Grätzel M (1991): Nature, 353, 737-740.

[3] Khalil E.J (2012): Sains malaysiana 41, 1011–1016.

[4] Bisquert J and Vikhrenko V. S (2004): Physics chemistry, B108, 2313-2322.

[5] Chen L.C (2015): Taipei, Taiwan, 1, 110-126.

[6] Kamat P (2012): Journal of Physical Chemistry Letters, 116, 11849–11851.

[7] Tang X.H, Zhang Y, Yin G.F, Zhou D.L, Liu H and Zheng C.Q (2004): Rare metal engineering, 33, 864–868.

[8] Tanaka K, Lapule M.F.V and Hisanaga T (1991): Chemical Physics Letters, 187, 73–76.

[9] Park J.Y, Lee C, Jung K.W and Jung D (2009): Bulletin of the Korean Chemical Society, 2 (30), 402-404.

[10] Linsebigler A.L, Lu G and Yates J.T (1995): Chemical Reviews, 95, 735–758.

[11] Addamo M, Bellardita M, Paola A.D and Palmisano L: (2006), Chemical Communications, 4943–4945.

[12] Qili C, Min L, Kaihua H and Bo L (2014), International Journal of Photoenergy, 2014, 1-7.

[13] Ibhadon A.O and Fitzpatrick P: (2013), Catalysts, 3 (1) 189-218.

[14] Tian F, Liu C, Zhao, Wang X, Wang Z and Yu C.J (2011): Journal of Computational Science and Engineering, 1, 33-41.

[15] Fujishima A and Honda K (1972): Nature, 238 (5358), 37–38.

[16] Navrotsky A (2011): Chem PhysChem, 12 (12), 2207–2215.

[17] Esch T.R Gadaczek I and Bredow T (2014): Applied Surface Science 288, 275– 287.

[18] Chen Q, Liu M, He K and Li B: (2004), Photoenergy, 2014, 1-7.

[19] Chen Q, Tang C and Zheng G (2009): Physical B, Condensed Matter, 404, 1074–1078.

[20] Labat F, Baranek P and Adamo C (2008): Journal of Chemical Theory and Computation, 4 (2), 341–352.

[21] Mino L, Ferrari A.M, Lacivita V, Spoto G, Bordiga S and Zecchina A (2011):, Journal of Physical Chemistry. C, 115 (15), 7694–7700.

[22] Clark S.J, Segall M.D, Pickard C.J, Hasnip P.J, M. J. Probert, Refson,M. C, Payne K, (2005): Zeitschrift fuer Kristallographie, 220(5-6). 567-570.

[23] Lin Y.M, Jiang Z.Y, Hu X.Y, Zhang X.D, Fan J, Miao H and Shang Y.B (2012): Chinese Physics. B, 21(3), 033103 -1-033103-6.